Published in final edited form as:

Immunohorizons. 2018 April 1; 2(4): 119–128. doi:10.4049/immunohorizons.1700064.

Clonal Bifurcation of Foxp3 Expression Visualized in Thymocytes and T Cells

Bonnie Yen[*,†], **Katherine T. Fortson**[*], **Nyanza J. Rothman**[*,†], **Nicholas Arpaia**[*], and **Steven L. Reiner**[*,†]

[*]Department of Microbiology and Immunology, College of Physicians and Surgeons of Columbia University, New York, NY 10032

[†]Department of Pediatrics, College of Physicians and Surgeons of Columbia University, New York, NY 10032

Abstract

Regulatory T cells (Tregs) are crucial for suppressing autoimmunity and inflammation mediated by conventional T cells. To be useful, some Tregs should have overlapping specificity with relevant self-reactive or pathogen-specific clones. Whether matching recognition between Tregs and non-Tregs might arise through stochastic or deterministic mechanisms has not been addressed. We tested the hypothesis that some Tregs that arise in the thymus or that are induced during Ag-driven expansion of conventional $CD4^+$ T cells might be clonally related to non-Tregs by virtue of asymmetric Foxp3 induction during cell division. We isolated mouse $CD4^+$ thymocytes dividing in vivo, wherein sibling cells exhibited discordant expression of Foxp3 and CD25. Under in vitro conditions that stimulate induced Tregs from conventional mouse $CD4^+$ T cells, we found a requirement for cell cycle progression to achieve Foxp3 induction. Moreover, a substantial fraction of sibling cell pairs arising from induced Treg stimulation also contained discordant expression of Foxp3. Division-linked yet asymmetric induction of Treg fate offers potential mechanisms to anticipate peripheral self-reactivity during thymic selection as well as produce precise, de novo counterregulation during $CD4^+$ T cell–mediated immune responses.

INTRODUCTION

Regulatory T cells (Tregs) are a $CD4^+$ T cell subset that expresses the X-linked transcription factor Foxp3 and plays an essential role in avoidance of autoimmunity and collateral tissue damage during immune responses. Deficiency of Foxp3, the major lineage-defining transcription factor of Tregs in mice (1–3) and humans (4), leads to fatal, multiorgan autoimmunity (1, 5, 6) known as immunodysregulation polyendocrinopathy enteropathy X-linked syndrome in humans (7–9).

Address correspondence and reprint requests to: Dr. Nicholas Arpaia and Dr. Steven L. Reiner, Columbia University, 701 W. 168th Street, HHSC 1208, New York, NY 10032. na2697@cumc.columbia.edu (N.A.) and sr2978@cumc.columbia.edu (S.L.R.). ORCIDs: 0000-0002-0657-0528 (N.A.); 0000-0002-1635-8619 (S.L.R.).

DISCLOSURES

The authors have no financial conflicts of interest.

During the development of thymic Tregs (tTregs), Foxp3 is induced in response to TCR signaling (10). Studies in TCR transgenic mice with expression of the cognate Ag have elucidated the important role of TCR specificity to self-antigen in the differentiation of tTregs (11–15). Furthermore, tTreg selection is promoted by a high degree of TCR affinity to self-antigen (11, 16–18). These findings are consistent with an instructive model of tTreg development, in which TCR affinities guide thymocyte cell fate (19). This model suggests that the range of TCR affinities to self-antigen that promote Treg development is higher than that which instructs positive selection of conventional T cells but less than that which induces negative selection.

Although TCR signaling is an important determinant in Treg development, other factors, such as costimulation through CD28 (20, 21) and cytokine signaling, have also been shown to play crucial roles (22–24). A two-step model suggests that in addition to a TCR-dependent phase of Treg selection that poises a Foxp3$^-$ CD25$^+$ Treg precursor cell to express Foxp3, there is also a subsequent TCR-independent phase, in which cytokine signaling, especially by IL-2, is crucial for the induction of Foxp3 expression (24, 25). It has been suggested that there is some TCR overlap between Tregs and conventional CD4 T cells (24, 26–32). Although selected single-positive thymocyte populations contain few proliferating cells, the characteristics of such minority subpopulations have not been fully interrogated (33, 34). We used confocal microscopy to visualize rare, dividing thymocytes that express Foxp3 and discovered a substantial frequency of sibling cells with discordant expression of Foxp3. Our results provide a potential explanation for how some convergence in the Ag receptor repertoire of self-reactive Tregs and non-Tregs might arise.

MATERIALS AND METHODS

Mice and in vitro Treg induction

Mice were housed under specific pathogen-free conditions and used in accordance with protocols approved by Columbia University's Institutional Animal Care and Use Committee and guidelines outlined by the National Institutes of Health. Thymi were isolated from 4- to 6-wk-old wild-type (WT) C57BL/6 and *Foxp3^{gfp}* (35) mice. Spleen and lymph nodes for in vitro induction cultures were isolated from 6- to 14-wk-old WT and *Foxp3^{gfp}* mice. Naive CD4$^+$ T cells were purified from spleens and lymph nodes by magnetic cell separation (Miltenyi Biotec) or cell sorting for CD4$^+$CD8$^-$TCRβ^{hi}CD25$^-$CD44^{lo}CD62L^{hi} cells on a FACSAria II cell sorter (BD Biosciences) prior to labeling with cell proliferation dye Cell Trace Violet (Thermo Fisher Scientific). Cells were cultured for 36 h at 5 ×10^5 cells per well in 48-well tissue culture plates precoated with anti-CD3 (1 μg/ml; BD Biosciences) and anti-CD28 (1 μg/ml; BD Biosciences) Abs, plus 100 U/ml recombinant human IL-2 (National Cancer Institute Biological Resources Branch) and 0.1 ng/ml recombinant human TGF-β (R&D Systems) in RPMI 1640 (Life Technologies) supplemented with 10% FBS (Gemini), 100 U/ml penicillin (Life Technologies), 100 U/ml streptomycin (Life Technologies), 100 μM nonessential amino acids (Life Technologies), 1 mM sodium pyruvate (Life Technologies), 2 mM GlutaMAX (Life Technologies), 10 mM HEPES (Life Technologies), and 55 μM 2-ME (Life Technologies). Cell cycle inhibitors were added at the start of cell culture: 2.5 mM L-mimosine (Sigma-Aldrich) and 5 or 10 μg/ml nocodazole (Cell Signaling

Technology). Ten micromolar cytochalasin B (Sigma-Aldrich) was added for the final 16 h of culture.

Flow cytometry

LIVE/DEAD Fixable Red or LIVE/DEAD Fixable Aqua (Invitrogen) staining was performed at 4°C or on ice for 15 min in PBS. Surface Ab staining was performed at 4°C or on ice for 20 min in PBS containing 2% FBS and 2 mM EDTA. For staining intracellular transcription factors, fixation and permeabilization was performed with the eBioscience Intracellular Fixation & Permeabilization Buffer Set Kit prior to intracellular staining for 1 h at 4°C or on ice. Abs for flow cytometry included CD4 (RM4-5; Invitrogen), CD8 (53-6.7; eBioscience), CD25 (PC61; BD Biosciences), CD44 (IM7; eBioscience), CD62L (MEL-14; BD Biosciences), and Foxp3 (FJK-16S; eBioscience). Cells were analyzed or sorted on LSR II, LSRFortessa, and FACSAria II flow cytometers (BD Biosciences) with BD FACSDiva software. Data analysis was performed using FlowJo v.10.2 (Tree Star). FACS data presented in Fig. 3 are gated on forward scatter and side scatter properties indicative of singlet lymphocytes and live $CD4^+CD8^-$(CD4SP) cells.

Confocal microscopy

Cells were seeded onto coverslips (Thermo Fisher Scientific) coated with poly-L-lysine (Sigma-Aldrich) and allowed to adhere briefly before fixation with 4% paraformaldehyde (Sigma-Aldrich), quenching with 50 mM NH_4Cl (Sigma-Aldrich), permeabilization with 0.3% Triton X-100 (Sigma-Aldrich), and blocking with 0.25% fish skin gelatin (Sigma-Aldrich) and 0.01% saponin (Sigma-Aldrich) in PBS. Abs include the following: rat anti–β-tubulin (YOL1/34; Abcam), rabbit anti-Foxp3 (C29H4; Cell Signaling Technology), mouse anti-GFP CF 488 (9F9.F9; Sigma-Aldrich), rat anti-CD25 (PC61; BioLegend), rabbit anti-Helios/ IKZF2 (Proteintech), goat anti-rat Alexa Fluor 488 (Life Technologies), goat anti-rat Alexa Fluor 568 (Life Technologies), and goat anti-rabbit Alexa Fluor 568 (Life Technologies). ProLong Gold Antifade Mountant with DAPI (Invitrogen) was used to mount coverslips and stain DNA. Cells were stained with primary Abs for 1 h at room temperature or 4°C overnight, followed by washing in blocking buffer. Secondary Abs were stained for 1 h at room temperature. Washes were done with blocking buffer. Images were acquired on a Zeiss LSM710 or Nikon Ti Eclipse inverted confocal microscope and processed using Fiji v2.0.0-rc-43/1.51q software (36). Transmitted light and tubulin images shown are of a single z-plane. DAPI, Foxp3, Helios, and CD25 images shown are sum slice projections. Integrated signal density for detected Ags in individual cells was calculated based on signal thresholds set relative to negative staining controls. Asymmetry of DAPI, Foxp3, and CD25 was calculated from projections as (integrated density daughter 1 − integrated density daughter 2) / (integrated density daughter 1 + integrated density daughter 2), with values over 0.2 considered asymmetric. Positive Helios expression was defined as having an integrated density over 20,000.

Statistics

Statistical analyses were performed using Prism (GraphPad). Significance between Foxp3 or CD25 asymmetry values versus DAPI asymmetry values was determined using two-tailed *t* tests for paired data. Significance for drug treatment effect on Foxp3 induction was

determined using repeated-measures one-way ANOVA with Dunnett posttest. The *p* values are specified in each figure legend.

RESULTS

tTregs may arise during an asymmetric cell division

We used GFP-Foxp3 fusion protein reporter mice, *Foxp3*^{gfp} (35), and confocal microscopy to study the characteristics of dividing Tregs in the thymus. CD4SP GFP$^+$ cells were sorted from thymus prior to fixation and fluorescent staining. To enrich for cells undergoing later stages of cell division in vivo, events with forward light scatter properties (area versus height) indicative of cell doublets were included (Fig. 1A).

During microscopy, we used a combination of criteria that have been shown to specifically discriminate between adjacent but unrelated cells and actual sibling cell pairs in telophase or cytokinesis (37). Bona fide sibling cell pairs contained a bridge structure evident by transmitted light and fluorescent tubulin staining as well as distinct nuclei within each lobe of the doublet. Among the doublets that met the criteria for being authentic sibling cells, we then assessed the signal of GFP-Foxp3 with a combination of anti-GFP staining and GFP emission within the same fluorescence channel. Of the cytokinetic pairs with at least one GFP$^+$ daughter cell, we found 74% had discordant expression of GFP-Foxp3 between daughters (Fig. 1B, 1C).

To ensure the phenomenon of asymmetric Foxp3 expression was not an artifact confined to *Foxp3*^{gfp} mice, we also examined thymocytes from WT mice. We sorted on CD4SP CD25$^+$ cells (Fig. 2A) to enrich for Tregs and Treg precursors (24). We found 74% of cytokinetic doublets with at least one Foxp3$^+$ cell had asymmetric expression of Foxp3 (Fig. 2B, 2C), similar to findings in reporter mice.

To determine whether sibling cell discordance in Foxp3 expression was a random, unregulated event, we examined another marker of Treg selection. Among Foxp3-discordant sibling cell pairs with detectable CD25 expression, almost every pair exhibited concordant asymmetry of CD25 and Foxp3 (Fig. 3A, 3B). The coordinate asymmetry of Foxp3 and CD25 further suggests that Treg fate is being transmitted unequally to sibling cells. Signal strength for Treg selection is likely to exceed that of conventional CD4$^+$ selection (19). Insofar as CD25 colocalizes to the proximal side of an immune synapse (38), the foregoing results suggest the possibility that a Treg-specified daughter cell may have arisen proximal to the peptide/MHC and/or cytokine-selecting signal, whereas its more weakly signaled sister cell may have arisen distal to the selecting signal.

Because the TCR repertoire of Tregs and conventional CD4$^+$ T cells is only partially overlapping, we tested the possibility that some of the conventional daughter cells arising from Foxp3-discordant sibling cell pairs may be destined for apoptosis by examining their expression of Helios, which marks both surviving Tregs and apoptosis-destined conventional CD4SP thymocytes (39). In Foxp3-discordant sibling cell pairs, 54% of Foxp3$^-$ daughter cells expressed Helios, whereas 46% of the Foxp3$^-$ daughter cells were coordinately Helios$^-$

(Fig. 3C, 3D). These findings suggest that some sibling cells of tTregs may die, whereas some may become conventional $CD4^+$ T cells.

Foxp3 induction may be cell cycle–dependent and transmitted unequally

Tregs may also arise in the periphery from naive CD4 T cells or in vitro from conventional CD4 T cells stimulated in the presence of TGF-β. To explore other modes of Treg generation, we extended our analyses to an in vitro induced Treg (iTreg) model. Naive *Foxp3*^{gfp} $CD4^+$ T cells were stimulated with plate-bound Abs against CD3 and CD28, plus IL-2 and TGF-β.

Under these conditions, the induction of Foxp3 did not become readily detectable until cell division commenced between 1 and 2 d following stimulation (Fig. 4A). Consistent with the correlation between cell division and gene expression, Foxp3 induction at 1.5 d following stimulation was substantially inhibited by drugs that arrest the cell cycle at the G1 (mimosine) or G2/M (nocodazole) phases (Fig. 4B, 4D). In contrast, cytochalasin B, which arrests cells after mitosis and during cytokinesis, had little effect on Foxp3 induction. Because there was also some reduction in CD62L expression and CD44 induction, we sought to determine whether the defect in Foxp3 induction imposed by cell cycle inhibitors was simply due to a nonspecific toxicity. Analyses restricted to $CD44^{hi}$-gated $CD4^+$ cells with normal viability suggested that defective Foxp3 expression was more likely due to the specific actions of cell cycle inhibition (Fig. 4C, 4E), which is consistent with the delayed induction of Foxp3 observed in freely cycling cells (Fig. 4A).

To determine whether our findings of asymmetric Foxp3 in dividing thymocytes also extended to iTreg differentiation, we examined the Foxp3 expression pattern of nascent sibling cells under iTreg stimulatory conditions. Of conjoined sibling pairs with at least one GFP^+ cell, 33%exhibited asymmetric inductionofGFP-Foxp3 (Fig. 5), confirming that the cell cycle–dependent induction of Foxp3 can be transmitted unequally in the late stage of cell division. Cells in metaphase and anaphase exhibited symmetrical distribution of Foxp3 protein (data not shown), suggesting that unequal signaling after telophase, rather than unequal inheritance of the preformed Foxp3 protein, is responsible for differential gene expression in sibling cells. Whether altered strength of the in vitro signaling conditions or some lack of an in situ polarity cue artificially contributes to a reduced frequency of Foxp3 asymmetry will require further exploration.

DISCUSSION

Many models of Treg development suggest that Treg selection is determined by the strength and specificity of the TCR to self-antigen (19). Thymocytes with low TCR affinities to selecting ligands undergo positive selection and develop into conventional CD4 T cells. Thymocytes with very high TCR affinities to self-antigen undergo negative selection as a mechanism to eradicate possibly autoreactive lymphocytes. Tregs may prevent autoimmunity by possessing overlapping specificity to self-antigen while remaining under the threshold for negative selection.

The finding of unequal expression of Foxp3 in both dividing thymocytes and $CD4^+$ T cells in Treg-inducing conditions suggests that some Tregs may arise as a result of asymmetric cell division. We speculate that strong TCR interactions accompanied by appropriate cytokine signaling (20–24), which are apparently required for Treg selection, may trigger cell division in the thymus at low frequency (33, 34). If induction of Tregs is cell cycle–dependent, then it is possible that a previously described mechanism that silences Foxp3 in a proportion of cells during cell division (40, 41) may be antagonizing stable induction in one of two daughter cells. Alternatively, the strength of a peptide/MHC or cytokine signal, such as IL-2, in the thymus may be transmitted unequally to daughter cells, resulting in discordant induction of Foxp3 expression, a possibility suggested by the prior discovery of CD25 polarity in $CD4^+$ T cells (38). Either model (unequal silencing of Foxp3 after initial induction or simply unequal induction of Foxp3) would serve to explain why some overlap exists between TCR repertoires of Tregs and conventional $CD4^+$ T cells (26–32) by enabling clones to yield a conventional $CD4^+$ T cell alongside a Treg sibling cell with an identical TCR. Either scenario would also serve to explain why thymocytes with transgenic TCRs bearing high affinity for a self-peptide would undergo simultaneous positive selection of both Treg and conventional $CD4^+$ T cell fates (11).

Based on the finding that some of the $Foxp3^-$ sibling cells appear to express Helios, we cannot exclude the possibility that some of the conventional $CD4^+$ sibling cells from asymmetric thymocyte divisions are destined for apoptosis by negative selection (39) rather than surviving as viable $CD4^+$ thymocytes. Nonetheless, a surviving Treg with specificity for self-antigen would still be of utility in anticipating nonkindred conventional T cells that have a different TCR but overlapping reactivity for the same self-antigen. It also remains to be determined whether peripheral Tregs that arise from conventional $CD4^+$ T cells during in vivo immune responses are the product of an asymmetric cell division in situ.

Lymphocyte effector and memory fate diversification has been suggested to occur as a result of asymmetric nutritive signaling (37, 42–45). Cellular metabolism also plays an important role in Treg differentiation and stability (46, 47). Future studies will be needed to determine whether unequal metabolic, cytokine, or another class of signaling plays a role in discordant expression of Foxp3 in dividing thymocytes and induced Tregs. Nonetheless, the ability to couple Foxp3 induction to an asymmetric division provides a possible templating mechanism to match the appropriate specificities of dominant tolerance.

Acknowledgments

This work was supported by National Institutes of Health Grants AI113365 and AI076458 (to S.L.R.) and AI127847 (to N.A.), Searle Scholars Program SSP-2017-2179 (to N.A.), and by the Charles Revson Foundation (to S.L.R.).

Abbreviations used in this article

CD4SP	$CD4^+CD8^-$
iTreg	induced Treg
Treg	regulatory T cell

tTreg	thymic Treg
WT	wild-type

References

1. Fontenot JD, Gavin MA, Rudensky AY. Foxp3 programs the development and function of CD4+CD25+ regulatory T cells. Nat Immunol. 2003; 4:330–336. [PubMed: 12612578]
2. Hori S, Nomura T, Sakaguchi S. Control of regulatory T cell development by the transcription factor Foxp3. Science. 2003; 299:1057–1061. [PubMed: 12522256]
3. Khattri R, Cox T, Yasayko SA, Ramsdell F. An essential role for Scurfin in CD4+CD25+ T regulatory cells. Nat Immunol. 2003; 4:337–342. [PubMed: 12612581]
4. Yagi H, Nomura T, Nakamura K, Yamazaki S, Kitawaki T, Hori S, Maeda M, Onodera M, Uchiyama T, Fujii S, Sakaguchi S. Crucial role of FOXP3 in the development and function of human CD25+CD4+ regulatory T cells. Int Immunol. 2004; 16:1643–1656. [PubMed: 15466453]
5. Brunkow ME, Jeffery EW, Hjerrild KA, Paeper B, Clark LB, Yasayko SA, Wilkinson JE, Galas D, Ziegler SF, Ramsdell F. Disruption of a new forkhead/winged-helix protein, scurfin, results in the fatal lymphoproliferative disorder of the scurfy mouse. Nat Genet. 2001; 27:68–73. [PubMed: 11138001]
6. Godfrey VL, Wilkinson JE, Russell LB. X-linked lymphoreticular disease in the scurfy (sf) mutant mouse. Am J Pathol. 1991; 138:1379–1387. [PubMed: 2053595]
7. Powell BR, Buist NRM, Stenzel P. An X-linked syndrome of diarrhea, polyendocrinopathy, and fatal infection in infancy. J Pediatr. 1982; 100:731–737. [PubMed: 7040622]
8. Bennett CL, Christie J, Ramsdell F, Brunkow ME, Ferguson PJ, Whitesell L, Kelly TE, Saulsbury FT, Chance PF, Ochs HD. The immune dysregulation, polyendocrinopathy, enteropathy, X-linked syndrome (IPEX) is caused by mutations of FOXP3. Nat Genet. 2001; 27:20–21. [PubMed: 11137993]
9. Wildin RS, Ramsdell F, Peake J, Faravelli F, Casanova JL, Buist N, Levy-Lahad E, Mazzella M, Goulet O, Perroni L, et al. X-linked neonatal diabetes mellitus, enteropathy and endocrinopathy syndrome is the human equivalent of mouse scurfy. Nat Genet. 2001; 27:18–20. [PubMed: 11137992]
10. Sekiya T, Kashiwagi I, Yoshida R, Fukaya T, Morita R, Kimura A, Ichinose H, Metzger D, Chambon P, Yoshimura A. Nr4a receptors are essential for thymic regulatory T cell development and immune homeostasis. Nat Immunol. 2013; 14:230–237. [PubMed: 23334790]
11. Jordan MS, Boesteanu A, Reed AJ, Petrone AL, Holenbeck AE, Lerman MA, Naji A, Caton AJ. Thymic selection of CD4+CD25+ regulatory T cells induced by an agonist self-peptide. Nat Immunol. 2001; 2:301–306. [PubMed: 11276200]
12. Apostolou I, Sarukhan A, Klein L, von Boehmer H. Origin of regulatory T cells with known specificity for antigen. Nat Immunol. 2002; 3:756–763. [PubMed: 12089509]
13. Knoechel B, Lohr J, Kahn E, Bluestone JA, Abbas AK. Sequential development of interleukin 2-dependent effector and regulatory T cells in response to endogenous systemic antigen. J Exp Med. 2005; 202:1375–1386. [PubMed: 16287710]
14. Kawahata K, Misaki Y, Yamauchi M, Tsunekawa S, Setoguchi K, Miyazaki J, Yamamoto K. Generation of CD4(+)CD25(+) regulatory T cells from autoreactive T cells simultaneously with their negative selection in the thymus and from nonautoreactive T cells by endogenous TCR expression. J Immunol. 2002; 168:4399–4405. [PubMed: 11970982]
15. Walker LSK, Chodos A, Eggena M, Dooms H, Abbas AK. Antigen-dependent proliferation of CD4+ CD25+ regulatory T cells in vivo. J Exp Med. 2003; 198:249–258. [PubMed: 12874258]
16. Moran AE, Holzapfel KL, Xing Y, Cunningham NR, Maltzman JS, Punt J, Hogquist KA. T cell receptor signal strength in Treg and iNKT cell development demonstrated by a novel fluorescent reporter mouse. J Exp Med. 2011; 208:1279–1289. [PubMed: 21606508]
17. Carter JD, Calabrese GM, Naganuma M, Lorenz U. Deficiency of the Src homology region 2 domain-containing phosphatase 1 (SHP-1) causes enrichment of CD4+CD25+ regulatory T cells. J Immunol. 2005; 174:6627–6638. [PubMed: 15905501]

18. Cozzo Picca C, Simons DM, Oh S, Aitken M, Perng OA, Mergenthaler C, Kropf E, Erikson J, Caton AJ. $CD4^+CD25^+Foxp3^+$ regulatory T cell formation requires more specific recognition of a self-peptide than thymocyte deletion. Proc Natl Acad Sci USA. 2011; 108:14890–14895. [PubMed: 21873239]
19. Hsieh CS, Lee HM, Lio CWJ. Selection of regulatory T cells in the thymus. Nat Rev Immunol. 2012; 12:157–167. [PubMed: 22322317]
20. Lohr J, Knoechel B, Kahn EC, Abbas AK. Role of B7 in T cell tolerance. J Immunol. 2004; 173:5028–5035. [PubMed: 15470046]
21. Tai X, Cowan M, Feigenbaum L, Singer A. CD28 co-stimulation of developing thymocytes induces Foxp3 expression and regulatory T cell differentiation independently of interleukin 2. Nat Immunol. 2005; 6:152–162. [PubMed: 15640801]
22. Fontenot JD, Rasmussen JP, Gavin MA, Rudensky AY. A function for interleukin 2 in Foxp3-expressing regulatory T cells. [Published erratum appears in 2006 *Nat. Immunol.* 7: 427.]. Nat Immunol. 2005; 6:1142–1151. [PubMed: 16227984]
23. Vang KB, Yang J, Mahmud SA, Burchill MA, Vegoe AL, Farrar MA. IL-2, -7, and -15, but not thymic stromal lymphopoeitin, redundantly govern CD4+Foxp3+ regulatory T cell development. J Immunol. 2008; 181:3285–3290. [PubMed: 18714000]
24. Lio CWJ, Hsieh CS. A two-step process for thymic regulatory T cell development. Immunity. 2008; 28:100–111. [PubMed: 18199417]
25. Burchill MA, Yang J, Vang KB, Moon JJ, Chu HH, Lio CWJ, Vegoe AL, Hsieh CS, Jenkins MK, Farrar MA. Linked T cell receptor and cytokine signaling govern the development of the regulatory T cell repertoire. Immunity. 2008; 28:112–121. [PubMed: 18199418]
26. Hsieh CS, Liang Y, Tyznik AJ, Self SG, Liggitt D, Rudensky AY. Recognition of the peripheral self by naturally arising CD25+ CD4+ T cell receptors. Immunity. 2004; 21:267–277. [PubMed: 15308106]
27. Hsieh CS, Zheng Y, Liang Y, Fontenot JD, Rudensky AY. An intersection between the self-reactive regulatory and non-regulatory T cell receptor repertoires. Nat Immunol. 2006; 7:401–410. [PubMed: 16532000]
28. Pacholczyk R, Ignatowicz H, Kraj P, Ignatowicz L. Origin and T cell receptor diversity of Foxp3+CD4+CD25+ T cells. Immunity. 2006; 25:249–259. [PubMed: 16879995]
29. Pacholczyk R, Kern J, Singh N, Iwashima M, Kraj P, Ignatowicz L. Nonself-antigens are the cognate specificities of Foxp3+ regulatory T cells. Immunity. 2007; 27:493–504. [PubMed: 17869133]
30. Wong J, Obst R, Correia-Neves M, Losyev G, Mathis D, Benoist C. Adaptation of TCR repertoires to self-peptides in regulatory and nonregulatory CD4+ T cells. J Immunol. 2007; 178:7032–7041. [PubMed: 17513752]
31. Fazilleau N, Bachelez H, Gougeon ML, Viguier M. Cutting edge: size and diversity of CD4+CD25high Foxp3+ regulatory T cell repertoire in humans: evidence for similarities and partial overlapping with CD4+CD25− T cells. J Immunol. 2007; 179:3412–3416. [PubMed: 17785774]
32. Wolf KJ, Emerson RO, Pingel J, Buller RM, DiPaolo RJ. Conventional and regulatory CD4+ T cells that share identical TCRs are derived from common clones. PLoS One. 2016; 11:e0153705. [PubMed: 27100298]
33. Penit C, Vasseur F. Phenotype analysis of cycling and postcycling thymocytes: evaluation of detection methods for BrdUrd and surface proteins. Cytometry. 1993; 14:757–763. [PubMed: 8243204]
34. Bautista JL, Lio CW, Lathrop SK, Forbush K, Liang Y, Luo J, Rudensky AY, Hsieh CS. Intraclonal competition limits the fate determination of regulatory T cells in the thymus. Nat Immunol. 2009; 10:610–617. [PubMed: 19430476]
35. Fontenot JD, Rasmussen JP, Williams LM, Dooley JL, Farr AG, Rudensky AY. Regulatory T cell lineage specification by the forkhead transcription factor foxp3. Immunity. 2005; 22:329–341. [PubMed: 15780990]

36. Schindelin J, Arganda-Carreras I, Frise E, Kaynig V, Longair M, Pietzsch T, Preibisch S, Rueden C, Saalfeld S, Schmid B, et al. Fiji: an open-source platform for biological-image analysis. Nat Methods. 2012; 9:676–682. [PubMed: 22743772]
37. Lin WHW, Adams WC, Nish SA, Chen YH, Yen B, Rothman NJ, Kratchmarov R, Okada T, Klein U, Reiner SL. Asymmetric PI3K signaling driving developmental and regenerative cell fate bifurcation. Cell Reports. 2015; 13:2203–2218. [PubMed: 26628372]
38. Maldonado RA, Irvine DJ, Schreiber R, Glimcher LH. A role for the immunological synapse in lineage commitment of CD4 lymphocytes. Nature. 2004; 431:527–532. [PubMed: 15386021]
39. Daley SR, Hu DY, Goodnow CC. Helios marks strongly autoreactive $CD4^+$ T cells in two major waves of thymic deletion distinguished by induction of PD-1 or NF-κB. J Exp Med. 2013; 210:269–285. [PubMed: 23337809]
40. Li X, Liang Y, LeBlanc M, Benner C, Zheng Y. Function of a Foxp3 cis-element in protecting regulatory T cell identity. Cell. 2014; 158:734–748. [PubMed: 25126782]
41. Feng Y, Arvey A, Chinen T, van der Veeken J, Gasteiger G, Rudensky AY. Control of the inheritance of regulatory T cell identity by a cis element in the Foxp3 locus. Cell. 2014; 158:749–763. [PubMed: 25126783]
42. Nish SA, Zens KD, Kratchmarov R, Lin WW, Adams WC, Chen YH, Yen B, Rothman NJ, Bhandoola A, Xue HH, et al. CD4+ T cell effector commitment coupled to self-renewal by asymmetric cell divisions. J Exp Med. 2017; 214:39–47. [PubMed: 27923906]
43. Lin WW, Nish SA, Yen B, Chen YH, Adams WC, Kratchmarov R, Rothman NJ, Bhandoola A, Xue HH, Reiner SL. $CD8^+$T lymphocyte self-renewal during effector cell determination. Cell Reports. 2016; 17:1773–1782. [PubMed: 27829149]
44. Adams WC, Chen YH, Kratchmarov R, Yen B, Nish SA, Lin WW, Rothman NJ, Luchsinger LL, Klein U, Busslinger M, et al. Anabolism-associated mitochondrial stasis driving lymphocyte differentiation over self-renewal. Cell Reports. 2016; 17:3142–3152. [PubMed: 28009285]
45. Pollizzi KN, Sun I-H, Patel CH, Lo Y-C, Oh M-H, Waickman AT, Tam AJ, Blosser RL, Wen J, Delgoffe GM, Powell JD. Asymmetric inheritance of mTORC1 kinase activity during division dictates CD8(+) T cell differentiation. Nat Immunol. 2016; 17:704–711. [PubMed: 27064374]
46. Delgoffe GM, Kole TP, Zheng Y, Zarek PE, Matthews KL, Xiao B, Worley PF, Kozma SC, Powell JD. The mTOR kinase differentially regulates effector and regulatory T cell lineage commitment. Immunity. 2009; 30:832–844. [PubMed: 19538929]
47. Wei J, Long L, Yang K, Guy C, Shrestha S, Chen Z, Wu C, Vogel P, Neale G, Green DR, Chi H. Autophagy enforces functional integrity of regulatory T cells by coupling environmental cues and metabolic homeostasis. Nat Immunol. 2016; 17:277–285. [PubMed: 26808230]

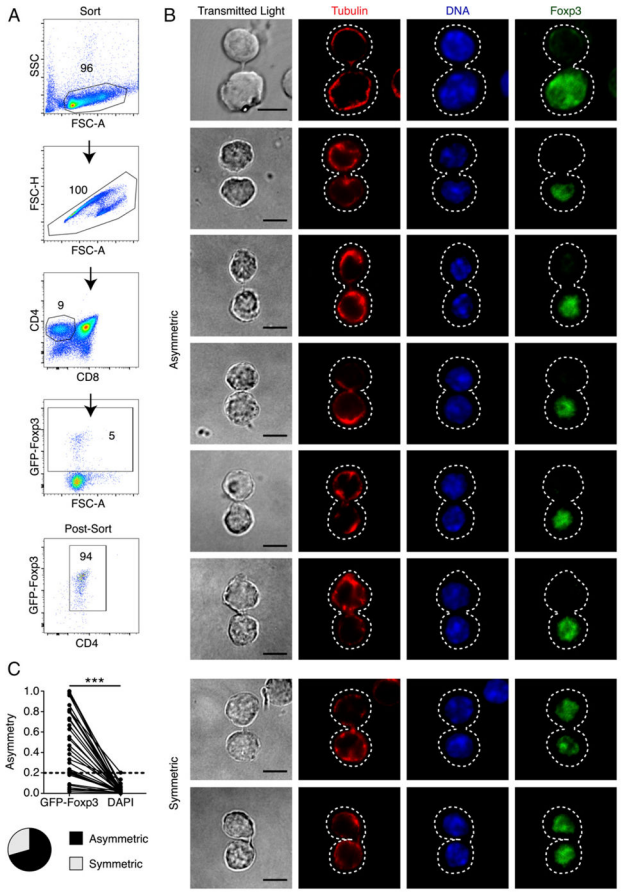

FIGURE 1. Discordant expression of Foxp3 reporter in sibling CD4SP thymocytes

(**A**) Sorting strategy applied to thymocytes from *Foxp3*^{gfp} mice: CD4^{+}CD8^{-}GFP^{+} cells, inclusive of doublets to prevent loss of cytokinetic pairs. The GFP^{+} gate was drawn generously to include cytokinetic pairs with unequal GFP-Foxp3 expression that may be measured as having intermediate intensity. (**B**) Conjoined sibling cells from sorted *Foxp3*^{gfp} thymocytes undergoing cytokinesis. Cells were stained with DAPI against DNA, anti–β-tubulin Ab, and anti-GFP Ab. Cytokinetic pairs were identified by initial visualization of β-tubulin staining of bridge between adjacent cells, followed by verification by transmitted light prior to evaluation of DNA and GFP-Foxp3. Signal shown in the “Foxp3” panel is both from GFP-Foxp3 and anti-GFP Ab. Top, Six representative sibling pairs with asymmetric GFP-Foxp3 expression. Bottom, Two representative sibling pairs with symmetric GFP-Foxp3 expression. Scale bar, 5 μm. (**C**) Top, Quantification of GFP-Foxp3 asymmetry in cytokinetic pairs with at least one GFP^{+} sibling (n = 34). Dotted line denotes asymmetry value of 0.2, where values >0.2 are considered asymmetric. Bottom, Pie chart summarizing frequency of cytokinetic pairs with asymmetric GFP-Foxp3 (74%). ***p < 0.0001 compared with DNA.

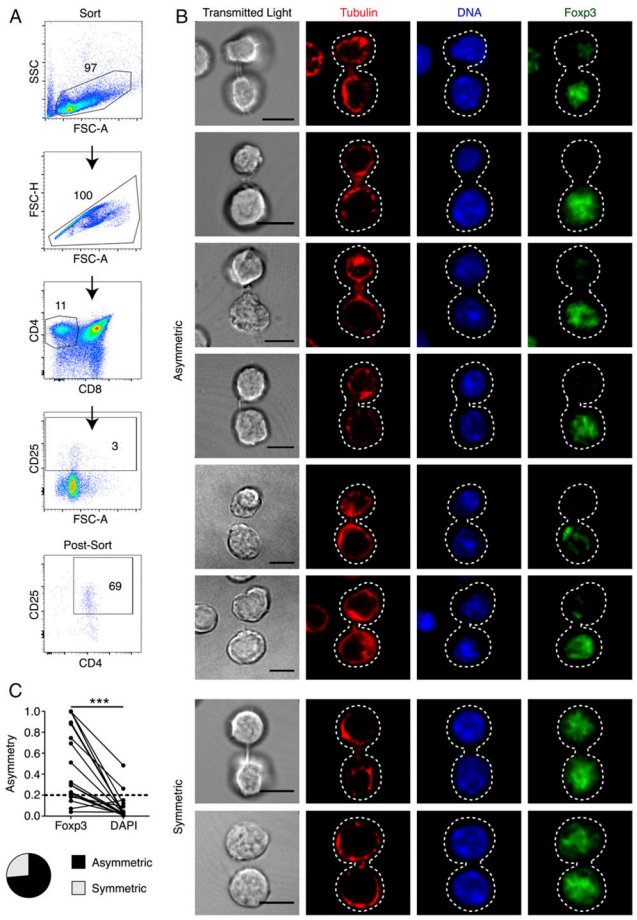

FIGURE 2. Discordant expression of Foxp3 in sibling CD4SP thymocytes

(**A**) Representative sorting strategy applied to thymocytes from WT mice: $CD4^{+}CD8^{-}CD25^{+}$ cells, inclusive of doublets. (**B**) Conjoined sibling cells from sorted WT thymocytes undergoing cytokinesis. Cells were stained with DAPI for DNA, anti–β-tubulin Ab, and anti-Foxp3 Ab. Top, Six representative sibling pairs with asymmetric Foxp3 expression. Bottom, Two representative sibling pairs with symmetric Foxp3 expression. Scale bar, 5 μm. (**C**) Top, Quantification of Foxp3 asymmetry in cytokinetic pairs with at least one $Foxp3^{+}$ sibling ($n = 19$). Dotted line denotes asymmetry value of 0.2, where values >0.2 are considered asymmetric. Bottom, Pie chart summarizing frequency of cytokinetic pairs with asymmetric Foxp3 (74%). ***$p < 0.0001$ compared with DNA.

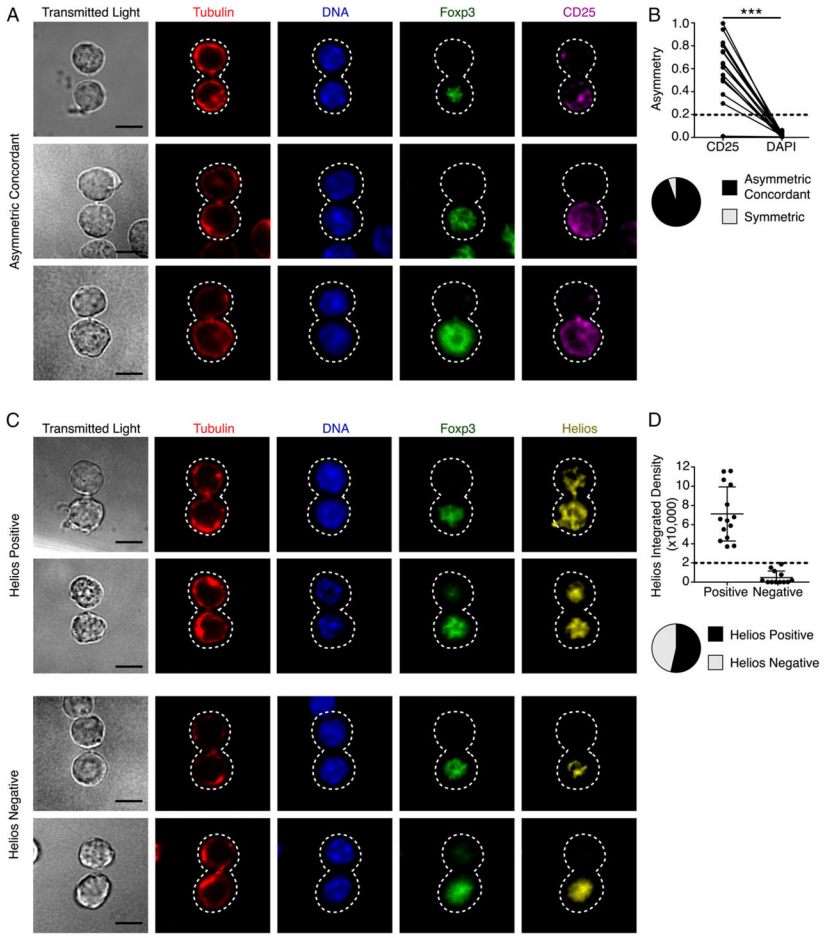

FIGURE 3. Concordant asymmetry of regulatory markers in sibling thymocytes

(**A**) CD4SP GFP^{+} cells inclusive of doublets were sorted from *Foxp3*^{gfp} thymocytes. Cells were stained with DAPI for DNA, anti–β-tubulin Ab, anti-Foxp3 Ab, and anti-CD25 Ab. Three representative sibling pairs with asymmetric Foxp3 expression and concordant asymmetry of CD25 abundance. Scale bar, 5 μm. (**B**) Top, Quantification of CD25 asymmetry in cytokinetic pairs with asymmetric Foxp3 expression and at least one CD25^{+} sibling ($n = 18$). Dotted line denotes asymmetry value of 0.2, where values >0.2 are considered asymmetric. Bottom, Among sibling pairs with asymmetric Foxp3 and detectable CD25 signal, 17 out of 18 pairs had concordant asymmetry of CD25 (94%); one sibling pair had symmetrical CD25. ***$p < 0.0001$ compared with DNA. (**C**) CD4SP CD25^{+} cells inclusive of doublets were sorted from *Foxp3*^{gfp} thymocytes. Cells were stained with DAPI for DNA, anti–β-tubulin Ab, anti-Foxp3 Ab, and anti-Helios Ab. Among sibling pairs with discordant Foxp3 expression, representative images wherein Foxp3^{-} sister was Helios^{+} (upper rows) or Helios^{-} (lower rows). (**D**) Top, Quantification of Helios abundance in the Foxp3^{-} sister of Foxp3-discordant sibling pairs ($n = 26$). Values greater and lower than 20,000 are considered positive and negative, respectively. Bottom, Among Foxp3-discordant sibling pairs, pie chart summarizing frequency of Foxp3^{-} sisters that were Helios^{+} (54%) or Helios^{-} (46%).

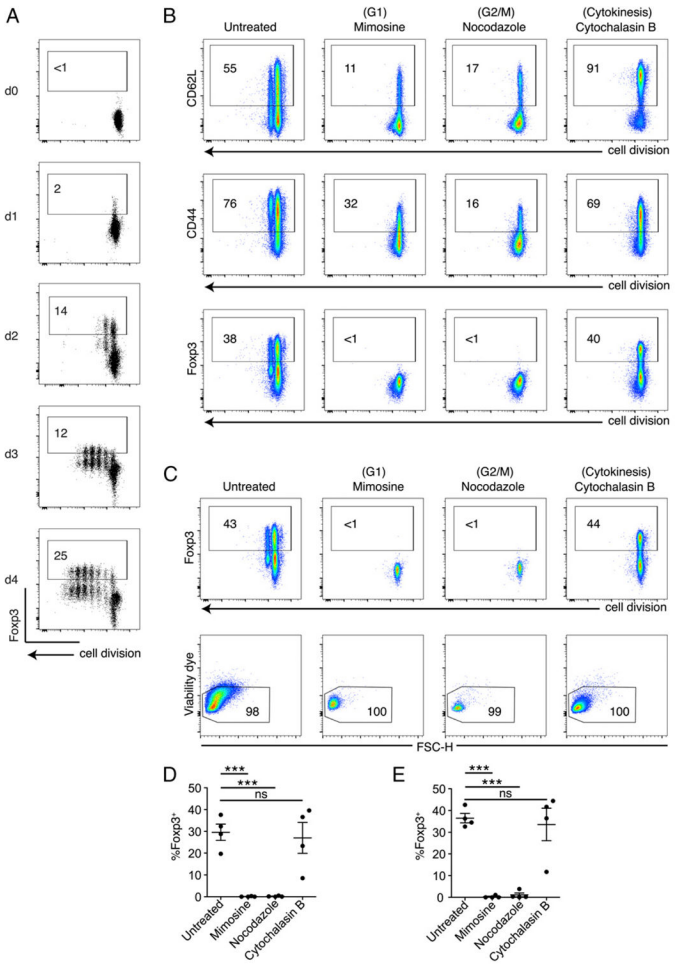

FIGURE 4. Foxp3 induction dependent on cell cycle progression in vitro

(**A**) Naive CD4 T cells were isolated from *Foxp3*^{gfp} mice, labeled with cell proliferation dye, and stimulated in vitro in Treg-inducing conditions prior to FACS analysis. Representative time course of Foxp3 expression versus cell division from day 0 to day 4 of culture. (**B** and **C**) Cells stimulated for 1.5 d were left untreated; treated initially with either Mimosine (2.5 mM) or Nocodazole (5 or 10 μg/ml); or treated for the final 16 h with Cytochalasin B (10 μM). (B) Representative FACS plots of cell proliferation dye versus indicated protein, gated on live CD4$^+$ lymphocytes. Foxp3 signal is the sum of GFP-Foxp3 emission plus anti-Foxp3 Ab staining. (C) Division, Foxp3 expression, cell size (forward light scatter [FSC-H]), and viability among CD44^{hi}-gated, CD4$^+$ lymphocytes. (**D**) Frequency of live CD4$^+$ lymphocytes expressing Foxp3 at day 1.5 of in vitro Treg induction ($n = 4$). ***$p = 0.0002$ compared with untreated. (**E**) Frequency of live CD44^{hi}CD4$^+$ lymphocytes expressing Foxp3 at day 1.5 of in vitro Treg induction ($n = 4$). ***$p < 0.0001$ compared with untreated.

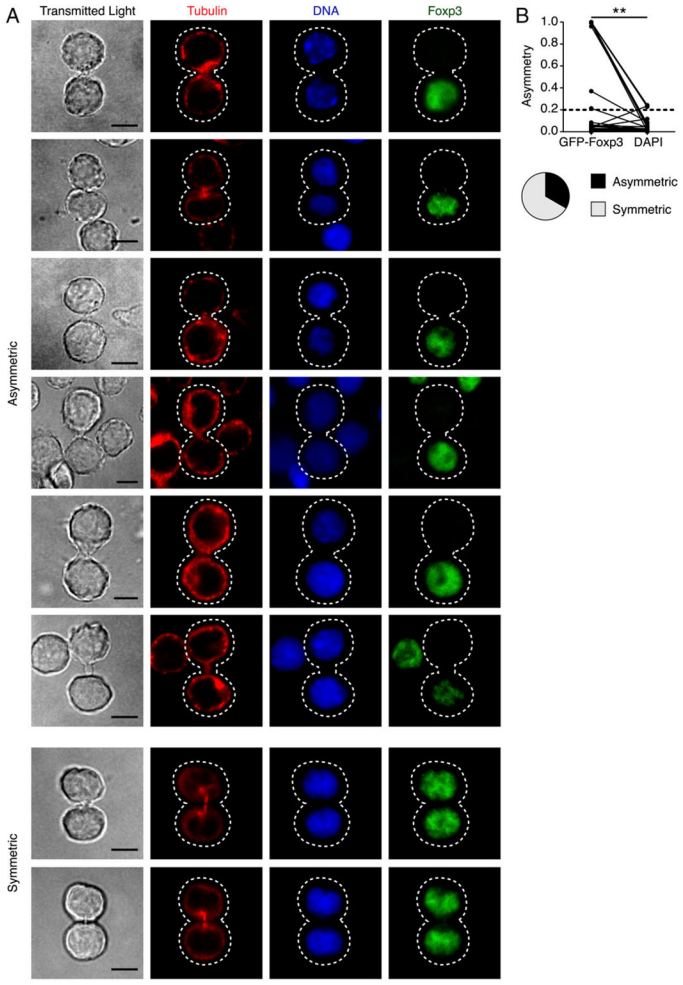

FIGURE 5. Discordant expression of Foxp3 in induced Tregs

(**A**) Naive CD4 T cells were isolated from *Foxp3*^{gfp} mice and stimulated in vitro for 1.5 d in Treg-inducing conditions prior to microscopy. Cells were stained with DAPI for DNA, anti–β-tubulin Ab, and anti-GFP Ab. Conjoined sibling cells from in vitro Treg induction culture undergoing cytokinesis. Signal shown in the Foxp3 panel is both from GFP-Foxp3 emission and anti-GFP Ab. Six representative sibling pairs with asymmetric GFP-Foxp3 expression and two representative sibling pairs with symmetric GFP-Foxp3 expression are shown. Scale bar, 5 μm. (**B**) Left, Quantification of GFP-Foxp3 asymmetry in cytokinetic pairs with at least one GFP$^+$ sibling (n = 30). Dotted line denotes asymmetry value of 0.2, where values ≥0.2 are considered asymmetric. Right, Pie chart summarizing frequency of cytokinetic pairs with asymmetric GFP-Foxp3 (33%). ** p = 0.0017 compared with DNA.